Titan's ionosphere: Model comparisons with Cassini Ta data

T. E. Cravens,[1] I. P. Robertson,[1] J. Clark,[1] J.-E. Wahlund,[2] J. H. Waite Jr.,[3] S. A. Ledvina,[4]
H. B. Niemann,[5] R. V. Yelle,[6] W. T. Kasprzak,[5] J. G. Luhmann,[4] R. L. McNutt,[7] W.-H. Ip,[8]
V. De La Haye,[3] I. Müller-Wodarg,[9] D. T. Young,[10] and A. J. Coates[11]

[1] On October 26, 2004, during its first encounter with Titan (Ta), the Cassini Orbiter moved from the dayside to the nightside with a closest approach altitude of 1174 km. In situ measurements of the main part of Titan's ionosphere were made by the Langmuir probe on the Cassini Radio and Plasma Wave Experiment (RPWS), while the Ion and Neutral Mass Spectrometer (INMS) measured the main constituents of the neutral atmosphere. The results of model calculations of Titan's ionosphere for Ta encounter conditions (e.g., near the terminator) are presented in this paper. The paper includes comparisons of calculated and measured electron densities along the spacecraft track. Ionization both by solar radiation and by incoming energetic electrons from Saturn's magnetosphere are needed to obtain good agreement between the measured and calculated electron densities. **Citation:** Cravens, T. E., et al. (2005), Titan's ionosphere: Model comparisons with Cassini Ta data, *Geophys. Res. Lett.*, *32*, L12108, doi:10.1029/2005GL023249.

1. Introduction

[2] Voyager 1 remotely measured an electron density profile in Titan's ionosphere in 1980 using the radio occultation technique [*Bird et al.*, 1997]. Many models of Titan's ionosphere have been constructed over the past decade or so [e.g., *Keller et al.*, 1992; *Banaskiewicz et al.*, 2000; *Galand et al.*, 1999; *Fox and Yelle*, 1997; *Wilson and Atreya*, 2004]. In the current paper we report on the results of a photochemical model that was described by *Keller et al.* [1992, 1998], *Gan et al.* [1992], and *Cravens et al.* [2004]. The first in situ measurements of the ionosphere were made in October 2004 by the Cassini RPWS experiment, which measured both the electron density and the temperature along the spacecraft track [*Wahlund et al.*, 2005]. In our current ionosphere model we use the molecular nitrogen and methane neutral density profiles measured during Ta by the Ion and Neutral Mass Spectrometer (INMS) onboard the Cassini Orbiter [*Waite et al.*, 2005]. The INMS did not make ion composition measurements during Ta, and we only report on the electron density model results in this paper.

[3] The Cassini Orbiter entered the upper atmosphere on the dayside and exited on the nightside during the Ta pass. The closest approach (CA) altitude of 1174 km is near the homopause but well below the exobase [*Waite et al.*, 2005]. The solar zenith angle (SZA) and latitude at CA were 91.1° and 41°, respectively. The CA location was about 90° from the sub-ram point on Titan (with respect to Saturn's magnetospheric flow direction), and the magnetic field was apparently draped around Titan [*Backes et al.*, 2005; *Ma et al.*, 2004]. Electrons residing in Saturn's magnetosphere must then travel along draped field lines (largely horizontal with respect to Titan's surface) to reach the atmosphere. The electron distributions measured by the Cassini Plasma Spectrometer (CAPS) experiment [*Young et al.*, 2004] in Saturn's outer magnetosphere at Titan's location had variable densities and temperatures with typical values of 0.1 cm^{-3} and 100 eV, respectively (CAPS paper in preparation, 2005).

[4] In order to investigate the ionospheric sources near CA, we constructed model ionospheres for different combinations of ionization sources: (1) only solar radiation, (2) only magnetospheric electrons (different incident electron spectra were tried), and (3) both solar and magnetospheric inputs. By comparing modeled electron density profiles with the density profile measured by Cassini we demonstrate the importance of magnetospheric electrons for the formation of the ionosphere. We also found, not surprisingly, that the calculated electron densities (n_e) are sensitive to ionospheric electron temperatures and to the incident solar irradiance level.

2. Model Description

[5] A description of the photochemical model of the ionosphere used for this paper can be found in *Keller et al.* [1992, 1998], *Gan et al.* [1992], and *Cravens et al.* [2004]. We adopt N_2 and CH_4 neutral density profiles (these are the major species) from INMS measurements made during the Ta encounter [*Waite et al.*, 2005]. The measured exospheric temperature was 149 K ± 3 K. The N_2 and CH_4 density profiles are similar to those measured by Voyager 1 in 1982 [*Smith et al.*, 1982; *Vervack et al.*, 2004; see *Waite et al.*, 2005]. The abundance of minor neutral species in the upper atmosphere strongly influences the ion composition

---

[1]Department of Physics and Astronomy, University of Kansas, Lawrence, Kansas, USA.

[2]Swedish Institute of Space Physics, Uppsala, Sweden.

[3]Department of Atmospheric, Oceanic, and Space Sciences, University of Michigan, Ann Arbor, Michigan, USA.

[4]Space Sciences Laboratory, University of California, Berkeley, California, USA.

[5]NASA Goddard Space Flight Center, Greenbelt, Maryland, USA.

[6]Lunar and Planetary Laboratory, University of Arizona, Tucson, Arizona, USA.

[7]Applied Physics Laboratory, Johns Hopkins University, Laurel, Maryland, USA.

[8]National Central University, Chung-Li, Taiwan.

[9]Space and Atmospheric Physics Group, Imperial College, London, UK.

[10]Southwest Research Institute, San Antonio, Texas, USA.

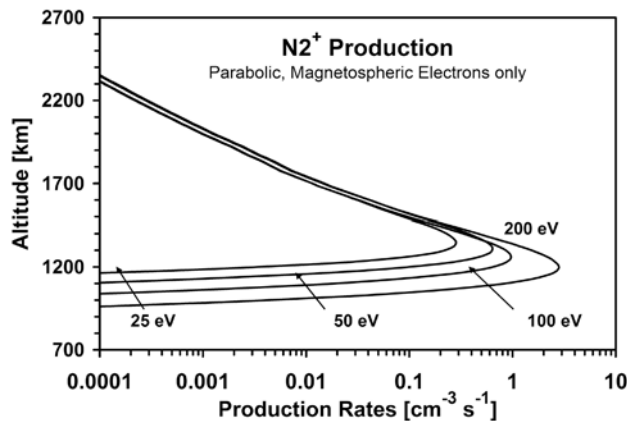[11]Mullard Space Science Laboratory, University College London, Holmbury St. Mary, Dorking, Surrey, UK.

Figure 1. Production rate profiles for N_2^+ ions for incident magnetospheric electron fluxes and for a parabolic magnetic field line configuration. The magnetospheric electron populations considered have electron densities and temperatures of: (n_e, T_e) = (0.1 cm^{-3}; 200 eV), (0.1 cm^{-3}; 100 eV), (0.2 cm^{-3}; 50 eV), (0.3 cm^{-3}; 25 eV).

but only weakly affects the total ion (or electron) density. The minor neutral abundances were adopted from *Toublanc et al.* [1995] [also see *Keller et al.*, 1998].

[6] The chemical scheme, described by *Keller et al.* [1998], includes more than 51 ion species and more than 300 chemical reactions. The electron density is the sum of the ion densities. The set of chemical equations is numerically solved at each altitude. The dominant ion species near the ionospheric peak are HCNH$^+$, C$_2$H$_5^+$, and heavy hydrocarbon ions. The details of the ion composition do not significantly affect the electron density because the dissociative recombination rate coefficients for the relevant polyatomic ion species are about the same. We estimate an electron density uncertainty due to this effect of $\approx$10% or less.

[7] We adopted the altitude-dependent electron temperatures (T_e) from the *Gan et al.* [1992] model. Near 1200 km this model predicted $T_e \approx 600$ K. The *Roboz and Nagy* [1994] model predicted $T_e \approx 1000$ K at this altitude. Both models showed very steep temperature gradients near this altitude. The T_e measured by the RPWS experiment near 1200 km was $\approx$1300 K. This range of temperatures can affect the electron density by about 25% (see the discussion section).

[8] The model includes ionization from both solar radiation and precipitating magnetospheric electrons. *Cravens et al.* [2004] presented ion production rates versus altitude and solar zenith angle for the solar ionization case, and the ion production rates in the current paper are very similar to these (for N_2^+ and CH$_4^+$), although some minor differences exist due to the new INMS neutral atmosphere adopted and due to a somewhat different solar irradiance spectrum. At higher altitudes, significant ionization persists in the model for SZA up to 110°, due to the large neutral scale height relative to the radius of Titan (i.e., $H/R_T \approx .02$; for Venus this ratio is $\approx 10^{-3}$).

[9] Solar extreme ultraviolet (EUV) and soft x-ray fluxes are known to be quite variable [cf. *Tobisca and Eparvier*, 1998; *Tobisca et al.*, 2000]. The solar activity level during late 2004 was generally low (F10.7 proxy indices less than

$\approx$100), but for the encounter date F10.7 was $\approx$138. We adopt solar EUV fluxes from the SOLAR2000 irradiance model with F10.7 $\approx$ 85 [*Tobisca et al.*, 2000]. *Maurellis et al.* [2000] described the soft x-ray part of the spectrum we use. This solar spectrum is denoted "Solar 1." We also used a solar spectrum (denoted "Solar 2") uniformly enhanced from Solar 1 by the F10.7 ratio of 138/85 = 1.6. Note that solar fluxes observed at Earth are not necessarily appropriate for Saturn and that solar EUV and x-ray fluxes exhibit complex time variations including solar rotational modulations. We will demonstrate that a solar flux enhancement of a factor of 1.6 results in a 25% increase in n_e.

[10] The model also includes ion production from suprathermal electrons (photoelectrons from photoionization or electrons from Saturn's magnetosphere). These electrons move along magnetic field lines that have been pushed into the ionosphere by the incident magnetospheric flow [cf. *Ledvina and Cravens*, 1998; *Ma et al.*, 2004]. Electron fluxes were calculated using the two-stream method [*Nagy and Banks*, 1970; *Gan et al.*, 1992, 1993]. Auger electrons due to K-shell ionization were also included [*Cravens et al.*, 2004].

[11] Two magnetic field line configurations were adopted – radial field lines or parabolic field lines, which approximately account for field-line draping around Titan (see the description by *Gan et al.* [1993]). We found that magnetospheric electrons penetrate more deeply into the atmosphere by about one scale height ($\approx$70 km) for the radial case than for the parabolic case. Results will be shown only for the parabolic case. Electron fluxes were measured in the outer magnetosphere both by Voyager [cf. *Schardt et al.*, 1984] and by the Cassini CAPS instrument [*Young et al.*, 2004]. The distribution is approximately Maxwellian with a density of $n_{e,mag} \approx 0.1$ cm^{-3} and a temperature of $T_{e,mag} \approx 100$ eV, although there were variations in these values. For our calculations we adopted incident electrons with temperatures of 25 eV, 50 eV, 100 eV, and 200 eV. N_2^+ production rates are shown in Figure 1. Not surprisingly, electrons penetrate deeper into the atmosphere for higher temperatures.

3. Results

[12] The photochemical model was used to generate vertical ion density profiles for solar zenith angles appropriate for the Cassini Orbiter trajectory at Ta. Only the calculated electron densities are shown in this paper.

[13] First, we present results from model runs with ionization only from incident magnetospheric electrons (i.e., solar radiation is turned off). Time histories of n_e along the spacecraft track are shown for four such cases (Figure 2). The Cassini CAPS measurements in the outer magnetosphere favor magnetospheric electrons with n_e = 0.1 and T_e = 100 eV (CAPS paper in preparation, 2005). The model electron density maxima for all these cases are located near (i.e., for the 200 eV case) or above the spacecraft CA altitude (1174 km). The peak density on the outbound track for both the RPWS measurements and the 100 eV model results is located 130 s after CA.

[14] Calculated electron densities for only solar ionization inputs (no magnetospheric electrons, but photoelectrons are included) and with RPWS electron temperatures are shown as vertical profiles (Figure 3) and as a time history (Figure 4). The inbound leg of the trajectory is on the dayside (negative times from CA) and the outbound leg is
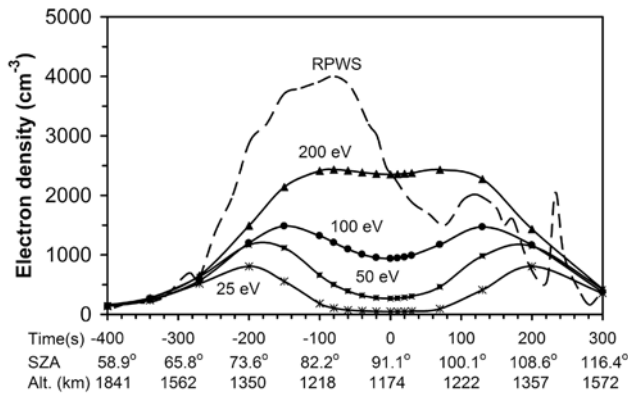
Figure 2. Time histories of the electron density along the Cassini Orbiter trajectory are shown for the 4 magnetospheric cases listed in Figure 1. Solar zenith angle and altitude along the track are also shown, but no ionization from solar radiation was included. Electron densities measured by the RPWS experiment [*Wahlund et al.*, 2005] are also shown.

on the nightside (positive times from CA). The maximum density along the track for both the RPWS data and the model is at t = −80 s (altitude z ≈ 1210 km; SZA ≈ 83°). These densities are $n_e \approx 3300$ cm^{-3} and 4000 cm^{-3} for the solar only model and the RPWS data, respectively (also see Table 1). The actual ionospheric peak in the model is located below the spacecraft for the dayside, although at CA (z = 1174 km; SZA = 91.1°), the track is near the model density peak. The RPWS data shows a second maximum on the outbound track (t ≈ +130 s), but the solar only model does not.

[15] The model was also run for both solar and magnetospheric inputs with Solar Flux 1 and the RPWS electron temperature profile (Figure 4). Overall, the model and the data are in agreement, particularly near the main maximum near t = −100 s. However, the model densities for times −20 s to +70 s somewhat exceed the measured densities,
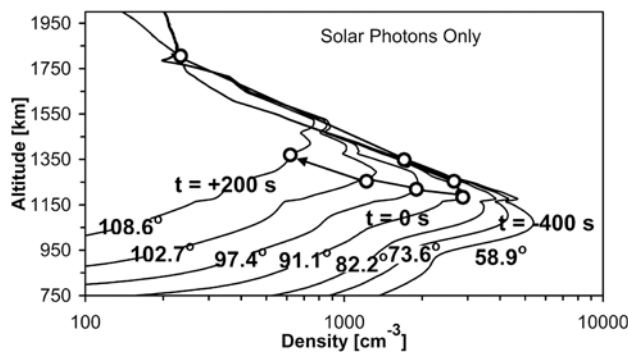

Figure 3. Calculated radial/vertical electron density profiles for solar ionization only (no magnetospheric electron contribution) and at several times (in units of seconds) and solar zenith angles for the Cassini Orbiter. The solar zenith angle varies from 58.9° (for t = −400 s) to 108.6° (t = +200 s). The solar zenith angle for closest approach (time t = 0 s) was 91.1°. The line and open circles indicate the relevant densities for the spacecraft track.
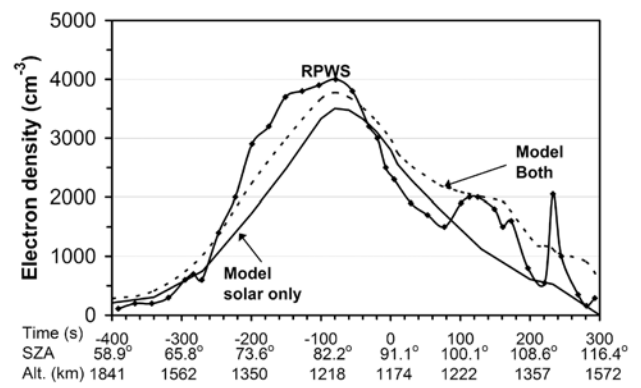

Figure 4. The same as Figure 2 but the model electron densities are for calculations for two cases: (1) ionization only by solar radiation (Solar Flux 1) and (2) ionization from both solar radiation (Solar Flux 1) and from incident magnetospheric electrons with a temperature of 100 eV.

and the model densities for t ≈ −150 s are somewhat too small. Furthermore, where the data shows a second maximum near t = +130 s (on the nightside), the model density only shows a ledge. The data also exhibits considerable small-scale structure at higher altitudes on the nightside and the model does not (discussed later).

[16] Table 1 tabulates electron densities for t = −100 s for a variety of model cases (including some not shown in Figures 1–4) and for RPWS. Model densities for the enhanced solar flux case (Solar Flux 2) are obviously higher than the Solar Flux 1 densities. And the densities calculated with the lower electron temperatures from *Gan et al.* [1993] are somewhat lower than the densities calculated using the higher RPWS temperatures. For the 3 cases listed for which both solar and magnetospheric inputs were included, the model density values in the table range from 3670 cm^{-3} to 4520 cm^{-3}; these values are within 15% of the measured density.

4. Discussion and Conclusions

[17] We obtained reasonable agreement between theoretical and measured electron density time histories only when the model included ionization both from solar radiation and from incident magnetospheric (suprathermal) electrons. Furthermore, we can account for about two-thirds of the maximum electron density measured by the RPWS Langmuir probe on the inbound (dayside) trajectory with only solar radiation, with magnetospheric electrons accounting for the remaining 33% contribution. However,

Table 1. Electron Densities at t = −100 s (Altitude of 1218 km and SZA = 82.2°)

Case	Electron Density (cm^{-3})
RPWS[a] n_e	3900
Magneto (100 eV; RPWS[a] T_e)	1320
Pure Solar (Solar 1; RPWS[a] T_e)	3300
Pure Solar (Solar 2; RPWS[a] T_e)	4100
Solar + Magneto (Solar 1; RPWS[a] T_e)	3670
Solar + Magneto (Solar 2; RPWS[a] T_e)	4520
Solar + Magneto (Solar 2; Gan[b] T_e)	3860

[a]*Wahlund et al.* [2005].
[b]*Gan et al.* [1993].

not surprisingly, the magnetospheric electron contribution to the ionosphere is much more important on the nightside (outbound).

[18] The model results also show some sensitivity (about $10-25\%$) to plausible variations (or uncertainties) in the solar flux and/or the electron temperature. A simple photochemical equilibrium expression for the electron density is: $n_e = [P/\alpha]^{1/2} = [P/\alpha_0]^{1/2} [T_e/300 \text{ K}]^{1/4}$, where P is the total ion production rate at a given location and where the effective dissociative recombination coefficient is given by $\alpha = \alpha_0(300 \text{ K}/T_e)^{1/4}$. The effective recombination coefficient near 1200 km estimated from the model is $\alpha_0 \approx 6 \times 10^{-7} \text{ cm}^3 \text{ s}^{-1}$. From this expression we can see why a factor of 1.6 higher solar flux (Solar Flux 1 and 2 cases) produces electron densities which are larger by a factor of $(1.6)^{1/2}$ (25%) (Table 1). Similarly, factors of 2 in the electron temperature produce factors of $(2)^{1/4}$ (19%) differences in the electron density.

[19] Small-scale structures evident in the measured electron density (e.g., the sharp peak at $t \approx +250$ s – outbound) were not reproduced by our model. However, the incident magnetospheric electron distribution in the model was independent of time, and it would not be surprising if the incident electron flux in the region of the magnetosphere linked to the ionosphere by the magnetic field varied with time. For example, magnetospheric flux tubes hung up in Titan's ionosphere for long times could be depleted of their electrons [cf. *Gan et al.*, 1993]. CAPS data should eventually shed more light on such time variations.

[20] Plasma transport effects (not included in this model) will also become important at higher altitudes (above about 1400–1500 km according to *Ma et al.* [2004] or *Cravens et al.* [1998]) where photochemical equilibrium ceases to be a good approximation. In this transport-dominated regime, the dynamical role of the magnetic field becomes important, as demonstrated by many MHD and hybrid models [e.g., *Cravens et al.*, 1998; *Ledvina and Cravens*, 1998; *Brecht et al.*, 2000; *Kabin et al.*, 1999; *Nagy et al.*, 2001; *Ma et al.*, 2004; *Ledvina et al.*, 2004].

[21] The current paper focused on the overall structure of Titan's ionosphere and the role of different ionization mechanisms. The next step will be to study the ion composition. The INMS and CAPS experiments just measured the ion composition in Titan's ionosphere during the T5 encounter in April 2005, and once it has been analyzed this composition data will allow us to more thoroughly test our understanding of the chemistry operating in Titan's ionosphere [e.g., *Keller et al.*, 1998; *Ma et al.*, 2004; *Fox and Yelle*, 1997].

References

Backes, H., F. M. Neubauer, M. K. Dougherty, H. Achilleos, N. Andre, C. S. Arridge, C. Bertucci, G. H. Jones, and K. K. Khurana (2005), Titan's magnetic field signature during the first Cassini encounter, *Science*, *308*, 992.

Banaskiewicz, M., et al. (2000), A coupled model of Titan's atmosphere and ionosphere, *Icarus*, *147*, 386.

Bird, M. K., R. Dutta-Roy, S. W. Asmar, and T. A. Rebold (1997), Detection of Titan's ionosphere from Voyager 1 radio occultation observations, *Icarus*, *130*, 426.

Brecht, S. H., J. G. Luhmann, and D. J. Larson (2000), Simulation of the Saturnian magnetospheric interaction with Titan, *J. Geophys. Res.*, *105*, 13,119.

Cravens, T. E., C. J. Lindgren, and S. A. Ledvina (1998), A two-dimensional multifluid MHD model of Titan's plasma environment, *Planet. Space Sci.*, *46*, 1193.

Cravens, T. E., J. Vann, J. Clark, J. Yu, C. N. Keller, and C. Brull (2004), The ionosphere of Titan: An updated theoretical model, *Adv. Space Res.*, *33*, 212, doi:10.1016/j.asr.2003.02.012.

Fox, J. L., and R. V. Yelle (1997), Hydrocarbon ions in the ionosphere of Titan, *Geophys. Res. Lett.*, *24*, 2179.

Galand, M., J. Lilensten, D. Toublanc, and S. Maurice (1999), The ionosphere of Titan: Ideal diurnal and nocturnal cases, *Icarus*, *104*, 92.

Gan, L., C. N. Keller, and T. E. Cravens (1992), Electrons in the ionosphere of Titan, *J. Geophys. Res.*, *97*, 12,136.

Gan, L., T. E. Cravens, and C. N. Keller (1993), A time-dependent model of suprathermal electrons at Titan, in *Plasma Environments of Non-Magnetic Planets*, COSPAR Colloq. Ser., vol. 4, edited by T. I. Gombosi, pp. 171–176, Elsevier, New York.

Kabin, K., T. I. Gombosi, D. L. DeZeeuw, K. G. Powell, and P. L. Israelevich (1999), Interaction of the Saturnian magnetosphere with Titan, *J. Geophys. Res.*, *104*, 2451.

Keller, C. N., T. E. Cravens, and L. Gan (1992), A model of the ionosphere of Titan, *J. Geophys. Res.*, *97*, 12,117.

Keller, C. N., V. G. Anicich, and T. E. Cravens (1998), Model of Titan's ionosphere with detailed hydrocarbon chemistry, *Planet. Space Sci.*, *46*, 1157.

Ledvina, S. A., and T. E. Cravens (1998), A three-dimensional MHD model of plasma flow around Titan, *Planet. Space Sci.*, *46*, 1175.

Ledvina, S. A., J. G. Luhmann, S. H. Brecht, and T. E. Cravens (2004), Titan's induced magnetosphere, *Adv. Space Res.*, *33*, 2092.

Ma, Y.-J., A. F. Nagy, T. E. Cravens, I. G. Sokolov, J. Clark, and K. C. Hansen (2004), 3-D global MHD model prediction for the first close flyby of Titan by Cassini, *Geophys. Res. Lett.*, *31*, L22803, doi:10.1029/2004GL021215.

Maurellis, A. N., T. E. Cravens, G. R. Gladstone, J. H. Waite Jr., and L. W. Acton (2000), Jovian X-ray emission from solar X-ray scattering, *Geophys. Res. Lett.*, *27*, 1339.

Nagy, A. F., and P. M. Banks (1970), Photoelectron fluxes in the ionosphere, *J. Geophys. Res.*, *75*, 6260.

Nagy, A. F., Y. Liu, K. C. Hansen, K. Kabin, T. I. Gombosi, M. R. Combi, and D. L. DeZeeuw (2001), The interaction between the magnetosphere of Saturn and Titan's ionosphere, *J. Geophys. Res.*, *106*, 6151.

Roboz, A., and A. F. Nagy (1994), The energetics of Titan's ionosphere, *J. Geophys. Res.*, *99*, 2087.

Schardt, A. W., K. W. Behannon, R. P. Lepping, J. F. Carbary, A. Eviatar, and G. L. Siscoe (1984), The outer magnetosphere, in *Saturn*, edited by T. Gehrels and M. S. Matthews, pp. 416–459, Univ. of Ariz. Press, Tucson.

Smith, G. R., et al. (1982), Titan's upper atmosphere: Composition and temperature from EUV solar occultation results, *J. Geophys. Res.*, *87*, 1351.

Tobisca, W. K., and F. G. Eparvier (1998), EUV97: Improvements to EUV irradiance modeling in the soft X rays and FUV, *Sol. Phys.*, *177*, 147.

Tobisca, W. K., T. Woods, F. Eparvier, R. Viereck, L. Floyd, D. Bouwer, G. Rottman, and O. R. White (2000), The SOLAR2000 empirical solar irradiance model and forecast tool, *J. Atmos. Sol. Terr. Phys.*, *62*(14), 1233.

Toublanc, D., et al. (1995), Photochemical modeling of Titan's atmosphere, *Icarus*, *113*, 2.

Vervack, J. R., B. R. Sandel, and D. F. Strobel (2004), New perspectives on Titan's upper atmosphere from a reanalysis of the Voyager 1 UVS solar occultations, *Icarus*, *170*, 91.

Wahlund, J.-E., et al. (2005), Cassini measurements of cold plasma in the ionosphere of Titan, *Science*, *308*, 986.

Waite, J. H., Jr., et al. (2005), Ion Neutral Mass Spectrometer (INMS) results from the first flyby of Titan, *Science*, *308*, 982.

Wilson, E. H., and S. K. Atreya (2004), Current state of modeling the photochemistry of Titan's mutually dependent atmosphere and ionosphere, *J. Geophys. Res.*, *109*, E06002, doi:10.1029/2003JE002181.

Young, D. T., et al. (2004), Cassini Plasma Spectrometer Investigation, *Space Sci. Rev.*, *114*, 1.

———————————
J. Clark, T. E. Cravens, and I. P. Robertson, Department of Physics and Astronomy, University of Kansas, Lawrence, KS 66045, USA. (cravens@ku.edu)

J.-E. Wahlund, Swedish Institute of Space Physics, S-75591 Uppsala, Sweden.

V. De La Haye and J. H. Waite Jr., Department of Atmospheric, Oceanic, and Space Sciences, University of Michigan, Ann Arbor, MI 48109, USA.

S. A. Ledvina and J. G. Luhmann, Space Sciences Laboratory, University of California, Berkeley, CA 94720, USA.

W. T. Kasprzak and H. B. Niemann, NASA Goddard Space Flight Center, Greenbelt, MD 20771, USA.

R. V. Yelle, Lunar and Planetary Laboratory, University of Arizona, Tucson, AZ 85721, USA.

R. L. McNutt, Applied Physics Laboratory, Johns Hopkins University, Laurel, MD 20723, USA.

W.-H. Ip, National Central University, Chung-Li 32054, Taiwan.

I. Müller-Wodarg, Space and Atmospheric Physics Group, Imperial College, London W1P 7PP, UK.

D. T. Young, Southwest Research Institute, P.O. Drawer 28510, San Antonio, TX 78228, USA.

A. J. Coates, Mullard Space Science Laboratory, University College London, Holmbury St. Mary, Dorking, Surrey RH5 6NT, UK.